Magneto-optical effects of excitons in BiI_3 crystals under pulsed high magnetic fields. II. Excitons localized at two-dimensional defects

T. Komatsu, K. Koike, and Y. Kaifu
Department of Physics, Faculty of Science, Osaka City University, Sumiyoshi-ku, Osaka 558, Japan

S. Takeyama, K. Watanabe,* and N. Miura
Institute for Solid State Physics, University of Tokyo, Roppongi, Minato-ku, Tokyo 106, Japan
(Received 2 March 1993)

Magneto-optical spectra for various types of excitons localized at two-dimensional (2D) defects in BiI_3 crystals were investigated in pulsed high magnetic fields up to 42 T. The localized excitons were observed as very sharp lines below the indirect exciton energy. For all these exciton transitions, we have observed common features such as very large anisotropy with respect to both the magnetic-field direction and the incident light polarization, characteristic energy shifts to high or low energy side with B^2 dependence, and growth of new lines with increasing fields. The observed magnetic-field effects were interpreted in terms of the Zeeman terms of cationic excitons perturbed by various kinds of stacking disorders that have 2D characters.

I. INTRODUCTION

Nonperiodic potentials due to various kinds of defects have generally large effects on excitons. Among these, excitons bound to point defects in semiconductors have been most extensively investigated. The magnetic-field effect gives detailed information not only on the localized states but also on the host exciton state. In semiconductors, most of the previous works concerning the magnetic-field effects on bound excitons have been done in low magnetic fields.[1] The magnetic-field effect depends on the values of the exciton mass and radius. As shown in a preceding paper,[2] internal structures of the small radius excitons in BiI_3 have been clarified by the measurement of magneto-absorption (MA) spectra in high magnetic fields. Excitons having small radii such as those in BiI_3 are strongly affected by crystal defects.

In layered crystals such as BiI_3, there exist two-dimensional (2D) defects created by various types of stacking disorders. The 2D defect itself has a two-dimensional translational symmetry which is different from the host crystal. In two-dimensional lattices, translational motion of such localized excitons is still possible. There have been only a few investigations on excitons localized in 2D defects.

The 2D defects destroy a lattice periodicity along the direction of the layer stacking. Normal stacking in BiI_3 crystals has a 3R ($\alpha\beta^A\gamma\alpha\beta^B\gamma\alpha\beta^C\gamma\cdots$) structure as denoted in the preceding paper, where α, β, and γ denote the three possible positions of the close-packed atom sites, and A, B, and C denote the three possible positions of the octahedral vacant of cation sites.[2] However, an inverse stacking of 3R′ ($\alpha\beta^A\gamma\alpha\beta^C\gamma\alpha\beta^B\gamma\cdots$) is often mixed in the normal stacking, which has been identified by the extra spots in the x-ray diffraction.[3] It should be considered that there exist various kinds of stacking faults at the boundary of the 3R and 3R′ structures during the crystal growth. It has been proposed that one of the most common native faults (growth fault) in BiI_3 corresponds to an interchange of the positions of cations and anions across the fault plane.[4] In addition to the bulk exciton transitions, various types of stacking disorders give rise to different exciton transitions which are localized in the 2D defects. In fact, fine structures due to such stacking disorders have been observed in the exciton spectrum in GaSe (Ref. 5) and PbI_2 (Ref. 6) crystals. There have been observed various types of characteristic exciton transitions related to such stacking disorders in BiI_3 crystals, as is explained in detail in the following.

Figure 1 shows the absorption spectra near the indirect edge for two different samples. For the sample shown in

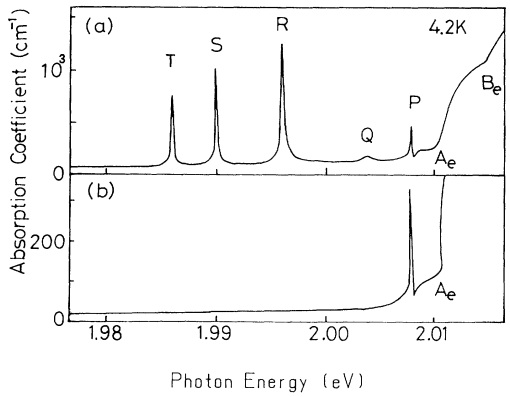

FIG. 1. The absorption spectra below the indirect edge at 4.2 K. (a) The spectrum for a sample showing the sharp P,Q,R,S, and T lines. (b) The spectrum for a sample showing only the P line. The P line is located very close to the indirect exciton energy E_{gx}^i. The Q,R,S, and T lines are ascribed to the stacking fault excitons. A_e and B_e indicate the A and B phonon-emission steps in the indirect transitions, respectively.

(a), sharp absorption lines are observed. They are denoted as P,Q,R,S, and T from a high-energy side. In some other samples, only the P line is observed as shown in (b). From such a sample dependence, the origin of the P line is considered to be different from that of the Q,R,S, and T lines. The P line appears very close to the indirect exciton energy E_{gx}^{i}. Karasawa, Komatsu, and Kaifu have shown by a resonant Raman scattering that a polytype structure folds back the Brillouin zone of the electronic states as well as the phonon states. The indirect exciton state at the Z point folds back to the Γ point and a direct exciton transition occurs at the same energy position as the indirect gap. The absorption intensity of the P line is observed to be very weak in comparison with that of the bulk direct exciton, which implies that the volume of a polytype in the host crystal is very small. The P line was considered as such a direct type exciton transition in a small volume of the polytype contained in the host crystal.[7]

The Q,R,S, and T lines are also observed in some type of samples.[8] At first, Gross, Perel, and Shekhmametev[9] proposed a bielectron (or bihole) model to interpret these lines, since the prominent P,R,S, and T lines (called $n=3,4,5$, and 6, respectively, in their notations) appeared as an inverse hydrogenlike series convergent to a long-wavelength side. However, the strong sample dependence of the absorption lines suggests that they should be attributed to some defects in origin, and various difficulties in the bielectron model have been pointed out.[10] By parallel investigations of spectroscopic and x-ray structure analysis, we proposed that the R,S, and T lines could be explained as exciton transitions in a planar lattice formed by a native stacking fault in BiI_3 crystals.[11]

The magnetic-field effects for the sharp lines corresponding to the R,S, and T lines in our notations have been investigated already by Gross, Uraltsev, and Shekhmamet'ev[12] to verify the bielectron model, but the effect was so small in low magnetic fields that a clear conclusion was not reached. Recently, Starostin *et al.*[13] have reported the results of similar measurements. They observed no Zeeman splitting, but a negative diamagnetic shift in magnetic fields up to 50 T. The negative diamagnetic shift has been analyzed theoretically by the bielectron model, and they made a quantitative explanation of their experimental results.[14] However, there are some puzzling points in their paper if compared with our results presented here. We have reported previously that the magneto-absorption spectra of the Q,R,S, and T lines are well interpreted by the model based on linear Zeeman effects of the cationic exciton perturbed by a stacking fault.[15] They were called the stacking fault excitons (SFE's). Preliminary results of the MA spectra of the P line have also been presented.[16]

In this paper, we present more detailed experimental results of the MA spectra of the SFE and P lines in BiI_3. The polarization dependence and the anisotropy with respect to the angle between the crystal axis and the magnetic field are systematically studied for the observed sharp transitions. We discuss the Zeeman effects on a basis of cationic excitons localized at specific stacking disorders.

II. EXPERIMENTAL RESULTS

A. Magneto-absorption spectra of stacking fault excitons

BiI_3 samples were prepared using the same method as in the previous paper.[3] For the MA spectra of the SFE's, samples having very sharp linewidth were carefully selected among many as-grown single crystals. The samples were immersed in a liquid-helium bath of a cryostat installed in a pulse magnet. The MA spectra were measured by the same system in the preceding paper[2] in pulsed high magnetic fields up to 42 T. The sample temperature was monitored by a calibrated AuFe: Chromel thermocouple placed in the vicinity of the sample.

Figure 2 shows the magnetic-field dependence of the MA spectra of the SFE lines measured by the use of an unpolarized light for the $[\mathbf{B}\perp\mathbf{z},\mathbf{k}\|\mathbf{z}]$ configuration at 4.2 K up to 40 T. The T line shifts to the lower-energy side with increasing magnetic fields. It should be noted that at the beginning of the increasing magnetic field the shift is very small, but at fields higher than 17 T, a sudden increase of the shift is observed. The magnitude of the shift is -1.20 meV at 40 T. The MA spectra around the S line exhibit complex fine structure consisting of a few peaks in high fields above 26 T.

The principal line shifts slightly toward lower energies as the field is increased, and a line (called N_1) appears at the higher-energy side of the principal peak. The N_1 line shifts toward higher energy as the field is increased. The R line does not show any shifts in a low-magnetic-field region, and at fields higher than 35 T there appears a peak at the higher-energy side of the R line. At a first glance, the R line seems to shift to the higher-energy side. How-

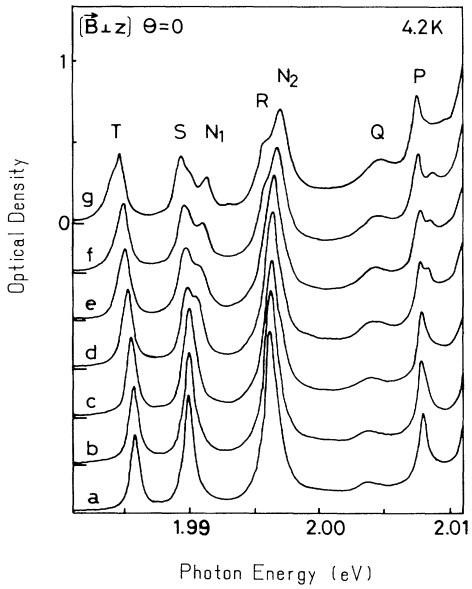

FIG. 2. The MA spectra of the SFE lines in the $\mathbf{B}\perp\mathbf{z}$ for $\theta=0$, where θ is the angle between the magnetic-field direction and the crystal a axis in a conventional hexagonal cell: curve a,$\mathbf{B}=0$ T; b,8.3 T; c, 17.3 T; d, 26.0 T; e, 30.9 T; f, 34.9 T; g, 40.4 T.

ever, as will be clarified later, it turns out that the R line is actually the one which shifts to lower energy, and the line which evolves and shifts to the higher-energy side is a line called the N_2 line. The Q line also shifts to the higher-energy side and increases its intensity with increasing field.

All the observed energy shifts of SFE lines are proportional to the square of the magnetic field, as shown in Fig. 3. It will be manifested later theoretically that the magnetic-field dependence of the SFE lines should be quadratic in the $[\mathbf{B}\perp\mathbf{z},\mathbf{k}\|\mathbf{z}]$ configuration. The coefficients of the $\mathbf{B}^2$ dependence are negative for the R,S, and T lines, while they are positive for the N_1,N_2, and Q lines. The absolute value of the coefficient of the $\mathbf{B}^2$ dependence for the T line is nearly equal to that for the N_1 line and that for the S line is nearly equal to that for the N_2 line. The extrapolated energy positions of the lines N_1 and N_2 at zero field do not coincide with those of the S and R lines at zero magnetic field, as shown in Fig. 3.

Figure 4 shows the dependence of the MA spectra on the angle θ between the magnetic field $\mathbf{B}$ and the crystal a axis in the conventional hexagonal cell for an unpolarized light at 4.2 K. The spectrum at $\mathbf{B}=0$ is shown by a broken line at the bottom for comparison. The spectra at 40 T are shown for different θ varied with a step of 30°. The T line at $\theta=0°$ shows a simple line shape, but a broad linewidth compared with that at $\mathbf{B}=0$. At $\theta=30°$ and 60°, the T line shows a line shape consisting of at least two components. At $\theta>60°$, each component changes its intensity drastically depending on the angle θ. The absorption intensity and peak position of each component change with θ. The linewidth becomes broader with increasing magnetic field as can be seen in Fig. 2. Similar angle dependence can be observed also in the other lines.

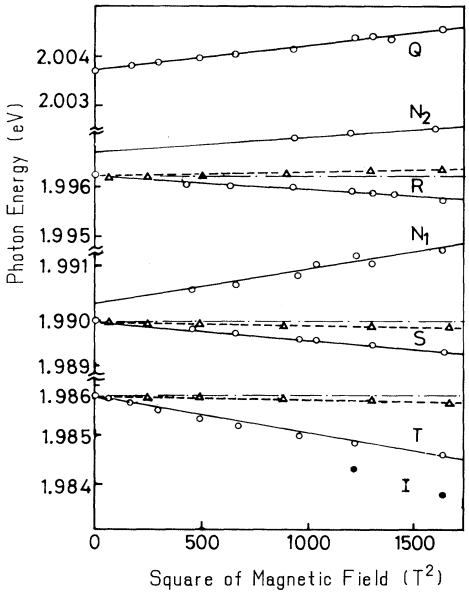

FIG. 3. Magnetic-field dependence of the energy for the SFE's in the $\mathbf{B}\perp\mathbf{z}$ (solid lines) and in the $\mathbf{B}\|\mathbf{z}$ (broken lines) configurations at 4.2 K, where open circles and triangles indicate the experimental points for each configuration. Solid circles indicate the energy position of the small structure which is observed near the T line at high magnetic fields. The values of energy shift depends on $\mathbf{B}^2$ and the sign of the shifts are negative for the T,S, and R lines and positive for the N_1,N_2, and Q lines in the $\mathbf{B}\perp\mathbf{z}$ configuration, while the shifts are negative for S and T lines and positive for the R line in the $\mathbf{B}\perp\mathbf{z}$ configuration. The dot-broken lines parallel to the lateral axis are indicated to assist the view of the small shift in the $\mathbf{B}\|\mathbf{z}$ configuration. The maximum error is indicated by the vertical bar.

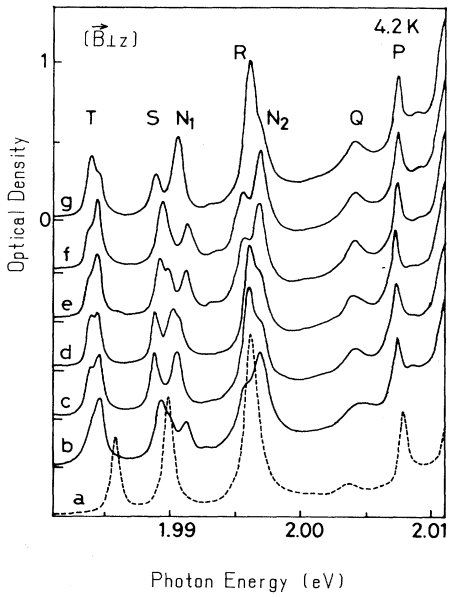

FIG. 4. The angle θ dependence on the MA spectra of the SFE's at 4.2 K in the $\mathbf{B}\perp\mathbf{z}$ configuration: the spectra indicated with solid lines are measured at about $\mathbf{B}=40$ T: curve a (broken line) is at $\mathbf{B}=0$ T; b, $\theta=0°$; $c,\theta=30°$; $d,\theta=60°$; $e,\theta=90°$; $f,\theta=120°$; $g,\theta=150°$.

As the SFE's originate from the bulk excitons localized at a stacking fault, we can expect the same polarization characteristics of SFE's as those of the bulk excitons, which is mentioned in the preceding paper.[2] From such a point of view, we examined the dependence of the spectra on the directions of the electric field $\mathbf{E}$ of the polarized light with respect to the magnetic field in the $[\mathbf{B}\perp\mathbf{z},\mathbf{k}\|\mathbf{z}]$ configuration. Figure 5 shows the dependence of the MA spectra of the SFE lines on the angle ϕ between $\mathbf{B}$ and $\mathbf{E}$ for the case of $\theta=0°$ and $\mathbf{B}=40$ T. The overall profile of the MA spectra measured with the polarized light shows common features with the unpolarized light. The peak energy of each SFE line does not depend on ϕ. However, the absorption intensity depends heavily on ϕ. At $\phi=0°$, the absorption intensity of the T line is increased in magnetic fields, while that of the S line decreases, and furthermore that of the R line is almost missing as shown in Fig. 5, curve b. On the other hand, the N_1 and N_2 lines take their maximum intensities at $\phi=0°$. Comparing the spectra b with a in Fig. 5, it is evident that the background absorption level around the Q line is increased

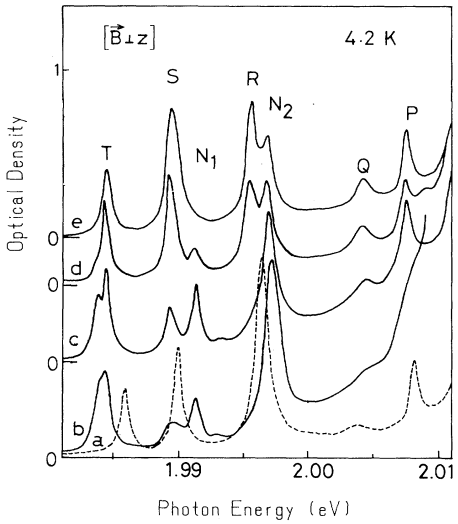

FIG. 5. The polarization angle ϕ dependence on the MA spectra of the SFE's at 4.2 K in the **B**⊥**z** configuration, where ϕ is the angle between magnetic field **B** and the electric field direction of a polarized light: The spectrum with the broken line is measured at **B**=0 T. Spectra with solid lines are measured at about 40 T; curve $b,\phi=0°$; $c,\phi=30°$; $d,\phi=60°$; $e,\phi=90°$.

with increasing field. This is ascribed to the magnetic-field-induced indirect exciton absorption, which has been discussed in detail in the preceding paper.[2] Taking account of this effect, we find that the Q line hardly changes its intensity even at 40 T in this configuration. When the angle ϕ is increased, the T line starts showing complicated structures. At $\phi=90°$ (Fig. 5, curve e), the T,N_1, and N_2 lines take the minimum intensities, while S,R, and Q lines take the maximum intensities, contrary to the case for $\phi=0°$. The relative absorption intensities of different

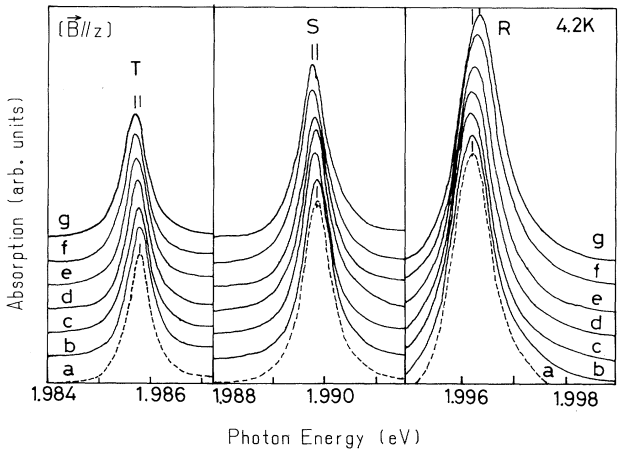

FIG. 6. The MA spectra of the SFE lines in the **B**‖**z** configuration at 4.2 K with unpolarized light: the vertical bars shown at the peaks indicate the energy separation between **B**=0 and 40 T; curve a (broken line), **B**=0 T; b,8.2 T; c,15.6 T; d,22.2 T; e,29.6 T; f,35.9 T; g,40.9 T.

SFE lines at **B**=**0** also depend on the angle between the polarization and the crystal axis.[17]

In Fig. 6, the MA spectra in the [**B**‖**z**,**k**‖**z**] configuration are shown for magnetic fields up to 40 T at 4.2 K. The peak energy shift in the **B**‖**z** is much smaller even at 40 T than in the case of the **B**⊥**z** configuration. The peak energy shift of the T line is −0.10 meV and that of the S line is −0.07 meV at 40 T. For the R line, a positive energy shift of +0.16 meV was observed. The spectra in the **B**‖**z** configuration are very different from those in the **B**⊥**z** configuration in many respects. The sign of the R line shift is opposite, and the amount of the shift of all lines is much smaller. The magnetic-field dependence of the shift is not linear as a function of **B**, but shows a quadratic form as shown by the broken lines in Fig. 3. These results clearly show a large anisotropy of MA with respect to the magnetic field.

B. MA spectra for the *P* line

In Fig. 7, the MA spectra for the P line are shown up to 40 T in different configurations: (a) [**B**⊥**z**,**k**‖**z**] with an unpolarized light, (b) [**B**⊥**z**,**E**⊥**B**,**k**‖**z**] with a polarized light, (c) [**B**⊥**z**,**E**‖**B**,**k**‖**z**] with a polarized light, (d) the [**B**‖**z**,**k**‖**z**] configuration with an unpolarized light. The splitting of the P line is not detected so distinctively in the [**B**⊥**z**,**k**‖**z**] configuration with the unpolarized light as shown in Fig. 7(a). However, components of the split lines P_1 and P_2 are observed selectively by using the polarized light as shown in Figs. 7(b) and (c). In the **E**⊥**B** configuration, the P line shifts to lower energy with increasing magnetic field. In the **E**‖**B** configuration, the P

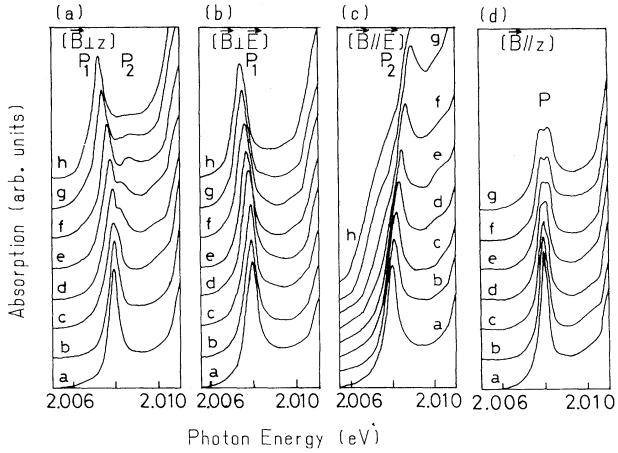

FIG. 7. The MA spectra of the P line at 4.2 K. (a) is measured in the [**B**⊥**z**,**k**‖**z**] configuration with unpolarized light: a,**B**=0 T; b,13.4 T; c,17.5 T; d,22.1 T; e,26.5 T; f,30.8 T; g,35.2 T; h,40.4 T. (b) is measured in the [**B**⊥**z**,**k**‖**z**] with the polarized light in the **E**⊥**z** configuration: a,**B**=0 T; b,12.9 T; c,17.0 T; d,21.9 T; e,25.6 T; f,30.4 T; g,37.2 T; h,40.0 T. (c) is measured in the [**B**⊥**z**,**k**‖**z**] with the polarized light in the **E**‖**z** configuration: a,**B**=0 T; b,13.5 T; c,17.3 T; d,21.7 T; e,25.5 T; f,30.4 T; g,37.0 T; h,40.0 T. (d) is measured in the [**B**‖**Z**,**k**‖**z**] configuration: a,**B**=0 T; b,15.6 T; c,22.2 T; d,29.6 T; e,35.9 T; f,38.4 T; g,40.9 T.

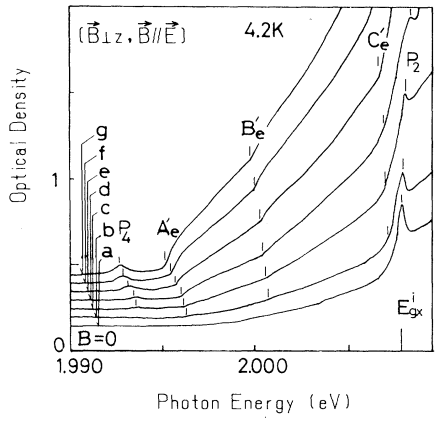

FIG. 8. MA spectra around the magnetic-field-induced indirect exciton transition in the [$\mathbf{B}\perp\mathbf{z},\mathbf{E}\|\mathbf{B}$] configuration: curve a,$\mathbf{B}=0$ T; b,11.3 T; c,15.8 T; d,22.2 T; e,29.5 T; f,35.9 T; g,41.0 T. A_e', B_e', and C_e' denote the energy position of phonon emission steps of the magnetic-field-induced indirect transition conserving their momenta in the transition with Ag-mode optical phonons, A, B, and C, respectively.

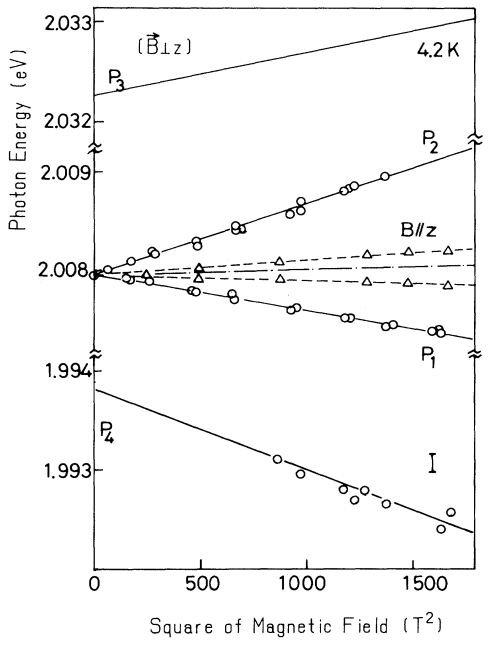

FIG. 9. Magnetic-field dependence of the peak energy for the P splitting lines at 4.2 K: the solid lines show the measurement in the $\mathbf{B}\perp\mathbf{z}$ configuration and the broken lines show that in the $\mathbf{B}\|\mathbf{z}$ configuration. The open circles and triangles indicate the experimental points in the $\mathbf{B}\perp\mathbf{z}$ and $\mathbf{B}\|\mathbf{z}$ configurations, respectively. The dot-broken line parallel to the lateral axis is indicated to assist the view of the small shift in the $\mathbf{B}\|\mathbf{z}$ configuration. The maximum error is indicated by the vertical bar.

line shifts to higher energy with increasing magnetic field. These observations confirm the splitting of the P line into two lines denoted by P_1 and P_2.

Figure 8 shows the MA spectra in the low-energy region of the P line in the $\mathbf{E}\|\mathbf{B}$ configuration. A peak which grows with increasing magnetic field is observed at a position located very close to the field-induced indirect exciton energy $E_{gx}^{i'}$. The peak which is induced with increasing magnetic field is called the P_4 line. The intensity of the P_4 line at 41.0 T is about 10% of that of the P line at zero magnetic field, and the situation is equivalent to the intensity relation between the field-induced indirect exciton at 40 T and the indirect exciton.[2] The intensity of the P_2 line becomes weaker with increasing magnetic field, while the intensity of the P_4 line increases with increasing magnetic field.

As shown in Fig. 7(d), a well-defined splitting of the P line is observed in the MA spectrum for the first time in the [$\mathbf{B}\|\mathbf{z},\mathbf{k}\|\mathbf{z}$] configuration at 4.2 K. The splitting at 40 T in this configuration is 0.4 meV. Thus it was found that the P line splits into two states under magnetic fields in the $\mathbf{B}\|\mathbf{z}$ configuration as well as in the $\mathbf{B}\perp\mathbf{z}$ configuration.

The energy of the P line versus $\mathbf{B}^2$ is plotted in Fig. 9, which shows that the field dependence of the shift of the P line is also quadratic in the $\mathbf{B}\perp\mathbf{z}$ configuration. The shift of the P_1 line is smaller than that of the P_2 and P_4 lines. The shifts of the lines are obtained to be $+1.2$ meV for the P_2 and -1.1 meV for the P_4 line, and -0.6 meV for the P_1 line at 40 T. The absolute values of the shifts for the P_2 and P_4 lines are nearly equal. The energy of the P_4 line extrapolated to zero magnetic field is estimated to be 1.9938 eV at 4.2 K.

III. DISCUSSION

A. The stacking fault exciton states

1. *Localized cationic excitons at a stacking fault*

The origins of the Q,R,S, and T lines have been assigned to localized excitons at stacking faults in the crystal.[3] In a previous paper, we proposed an SFE model.[12] The stacking fault is produced by a translation of all the molecular positions by $\mathbf{t}=(\mathbf{a}+\mathbf{b})/3$ from the normal lattice site, where $\mathbf{a}$ and $\mathbf{b}$ are the unit vectors of the conventional hexagonal unit cell. Such stacking faults in the BiI_3 lattice corresponds to an interchange of the positions of the cations and anions across the fault plane. There are two kinds of deformations concerning the relative positions of the cations in a unit cell containing the stacking fault plane. One is weakly deformed and the other is strongly deformed. The former deformation occurs twice as frequently as the latter one. The two kinds of deformed cells are shown in Fig. 10(a) to be compared with the regular lattice. Since the ground-state wave functions of the exciton are confined nearly in one unit cell, it is expected that the deformation perturbs the ground state of the bulk excitons ψ_j and produces exciton states localized at the stacking fault, as shown in Figs. 10(b) and 10(c).

As mentioned in the preceding paper,[2] the band-edge

exciton states consist of four bonding states of the cationic exciton in the unit cell. These states are affected by two kinds of deformations in the unit cell arising from one stacking fault plane. This would result in two kinds of energy shifts and splittings of the degenerate cationic exciton states. The wave functions of SFE's can be constructed by linear combination of all the K_z (wave vector parallel to the z axis) components from the direct to the indirect states. Though the rate of the indirect exciton component is larger for the SFE state than the direct ones, we will not indicate any superscripts for distinguishing the indirect and the direct excitons in the description of the cationic states ψ's.[2] These states are denoted as ψ_3, ψ_4, ψ_6, and ψ_{10}. Theoretically, eight states are expected to exist due to the two kinds of stacking fault effects; however, six lines are actually observed, the Q, R, S, T lines, and the N_1 and N_2 lines which develop under magnetic fields. Therefore, there are degenerate lines among the lines associated with the strongly and weakly deformed states. From the resonant Raman scattering studies on the SFE lines, the R line can be regarded as a degenerate line.[17] Since the Q line is relatively broad compared with the other lines, we suppose that the Q line consists of nearly degenerate Q_1 and Q_2 states which arise from both types of deformations.

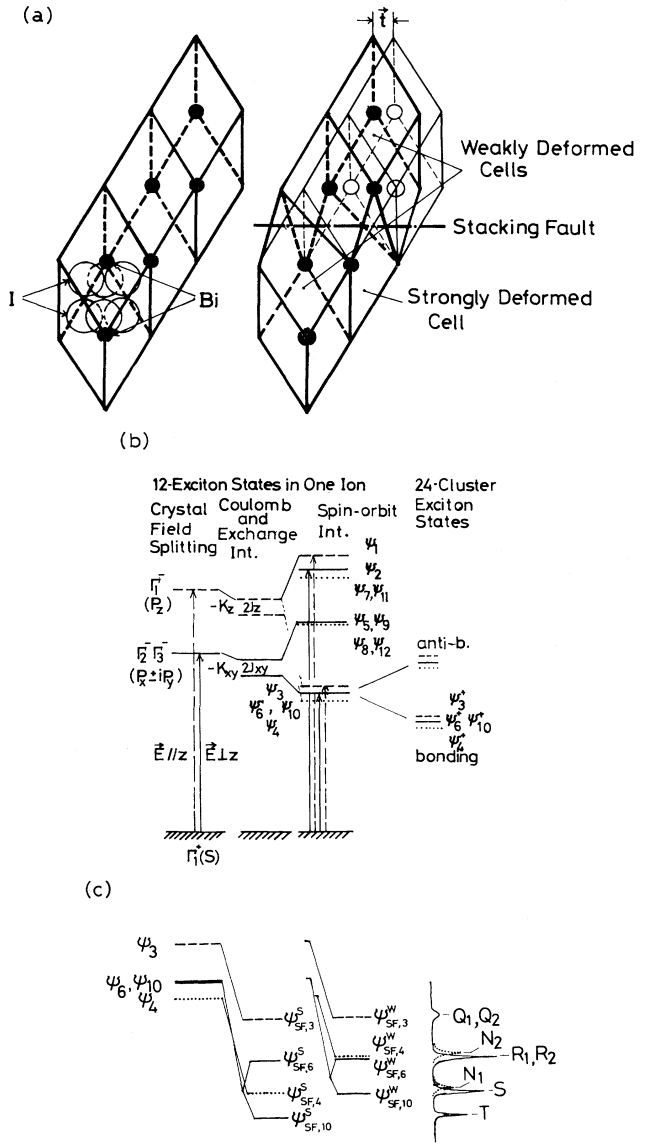

FIG. 10. (a) Three unit cells in regular stacking (left side) and two kinds of deformed cells at a stacking fault plane with the regular stacking (right side). Except one unit cell, only Bi ions in the unit cells are indicated by small circles. (b) The energy states of the bulk cationic excitons ψ_j in C_{3i} symmetry. (c) The energy states of the SFE $\psi^m_{\mathrm{SF},j}$: the band-edge cationic exciton states ψ_j are perturbed by two kinds of the deformed cells; the right figure shows the spectra of the SFE lines without magnetic field (solid line) and those in a magnetic field (dotted line).

The Q_1, R_1, N_1, and T lines correspond to $\psi^s_{\mathrm{SF},3}, \psi^s_{\mathrm{SF},6}, \psi^s_{\mathrm{SF},4}$ and $\psi^s_{\mathrm{SF},10}$ states and the Q_2, R_2, N_2, and S lines to $\psi^w_{\mathrm{SF},3}, \psi^w_{\mathrm{SF},6}, \psi^w_{\mathrm{SF},4}$, and $\psi^w_{\mathrm{SF},10}$ states, respectively, where the suffixes s and w denotes the states associated with the strong and the weak stacking fault effects. The energy states of SFE's are shown in Fig. 10(b) together with observed spectrum in magnetic field.

The ith ($i=3, 4, 6, 10$) SFE state can be expressed by a linear combination of the bulk exciton wave functions,

$$\psi^m_{\mathrm{SF},i} = \sum_j a^m_{ij} \psi_j \ , \tag{1}$$

where m refers to the unit cells deformed strongly or weakly by the stacking fault and j is taken to be 3, 4, 6, and 10. In Eq. (1), it may be reasonable to exclude the mixing of the triplet state $j=4$ with other states, because no tripletlike line is observed in zero magnetic field. The coefficients a^m_{ij} can be described by the matrix element $\langle \psi_i | H^m_{\mathrm{SF}} | \psi_j \rangle$ of the stacking fault effects between i and j of the bulk exciton states. The analytical form of the interaction Hamiltonian of the stacking fault effects H^m_{SF} is not known, but we can treat the matrix element as a parameter to be fitted to the energy positions of the SFE lines. The energy of the SFE's can be obtained by the perturbation treatment,

$$E^m_{\mathrm{SF},i} = E_i + \langle \psi_i | H^m_{\mathrm{SF}} | \psi_i \rangle + \sum_j \frac{|\langle \psi_i | H^m_{\mathrm{SF}} | \psi_j \rangle|^2}{E_i - E_j} + \cdots \ . \tag{2}$$

The first term E_i is the bulk exciton energy of each corresponding state which lies somewhere between the indirect and direct exciton energy. The second term should be negative as the SFE's appear at the low-energy side of the indirect excitons. Thus the energy positions for the SFE lines can be calculated by adjusting the parameters so that they are in agreement with the experimental result. It is found that the Q lines are mainly composed of z-like orbital with a mixture of a small portion of $(x \pm iy)$-like orbitals. The increase of absorption intensities of the Q line has been observed with increasing angle of the incident p-polarized light (**E** is parallel to the incident plane). The Q lines are weakly allowed in the **E**⊥**z** configuration even at a normal incidence to the layer

plane.[17] The R,S, and T lines are dipole allowed in the $\mathbf{E}\perp\mathbf{z}$ configuration.

The polarization characteristics of the R line is different from the S and T lines: it is found that the dipole direction of the R transition is perpendicular to that of the S and T transitions.[17] The observed absorption intensity ratio among the SFE lines is $R:S:T=4:2:1$. On the other hand, the degree of degeneracy according to the model provides the relation of $R:S:T=3:2:1$. These discrepancies can be attributed to some differences of the transition dipole matrix elements among these states. The present model of the cationic excitons perturbed by a stacking fault can well explain the overall characteristics of the absorption spectra of these SFE lines.

2. *The magnetic-field effects on the stacking fault excitons*

The magnetic-field effect on the SFE states can be calculated by the perturbation method, taking the SFE state as unperturbed states and linear Zeeman terms as the perturbation. Nonzero off-diagonal matrix elements $\langle\psi^m_{\mathrm{SF},i}|H_{\mathrm{Zeeman}}|\psi^m_{\mathrm{SF},j}\rangle$ cause a mixing among the SFE states. The energy of the ith state of the SFE in magnetic field $\mathbf{B}$ is given by the following equation up to the second-order:

$$E^m_{\mathrm{SF},i}(\mathbf{B})=E^m_{\mathrm{SF},i}(\mathbf{B}=\mathbf{0})+\alpha^m_i B_{\parallel}+\beta^m_i \mathbf{B}_{\perp}+\sum_j \gamma^m_{ij}\mathbf{B}^2_{\parallel}+\sum_j \delta^m_{ij}\mathbf{B}^2_{\perp}\ldots, \tag{3}$$

where $\alpha^m_i,\beta^m_i,\gamma^m_{ij}$, and δ^m_{ij} contain coefficients of the spin-orbit interaction, the g factor of electrons and holes and a sum of orbital quantum numbers, Bohr magneton μ_B, etc. The suffices i and j denote the states of the SFE, m is a suffix describing s or w. $\mathbf{B}_{\parallel}$ and $\mathbf{B}_{\perp}$ are the magnetic-field components parallel and perpendicular to the z axis, respectively. The expression for δ^m_{ij} is given by

$$\delta^m_{ij}=\sum_j \frac{(g^m_{\perp,j}\mu_B)^2 f(\theta)^2}{E^m_{\mathrm{SF},i}(\mathbf{0})-E^m_{\mathrm{SF},j}(\mathbf{0})}\ . \tag{4}$$

The $g^m_{\perp,j}$ is the effective g value in the $\mathbf{B}\perp\mathbf{z}$ configuration. The $f(\theta)$ is a function of the angle θ between the magnetic field and the crystalline axis $\mathbf{a}$ in the layer. This θ dependence originates from the xy component of the operator in the Zeeman terms. In the following, we will show that the present results of the MA spectra can be explained in the framework of the SFE model mentioned above. From the experimentally observed small $\mathbf{B}^2_{\parallel}$ dependence of the R,S, and T lines and the lack of a linear term in the $\mathbf{B}\perp\mathbf{z}$ configuration as shown by the broken lines in Fig. 3, the second term in (3) should be very small. The coefficient β in the third term also should be small in high magnetic fields according to the experimental results. The fourth term in Eq. (3) is expressed by a form similar to Eq. (4), but γ does not contain the function $f(\theta)$. Experimentally, the R line shifts toward higher energy, whereas the T line shifts to a lower side in the $\mathbf{B}\parallel\mathbf{z}$ configuration. This is explained by the difference of the sign of the coefficient γ^m_{ij} in Eq. (3); namely, the coefficient is positive for the R line and negative for the T line due to the sign of the energy denominator in an expression for γ^m_{ij} similar to Eq. (4). The coefficient of the S line is also negative since the S line is located at the lowest energy owing to the weak stacking fault effect in the SFE model, and the sign of the shift is determined dominantly by the energy denominator. As the shift in the $\mathbf{B}\parallel\mathbf{z}$ configuration is very small, the dominant term in Eq. (3) is the fifth term δ in the $\mathbf{B}\perp\mathbf{z}$ configuration. In the case of the $\mathbf{B}\perp\mathbf{z}$ configuration, a similar behavior can be expected from Eq. (4). This explains the following results: the shift is positive for the N_1 line while negative for the T line and the absolute value of the shift for the N_1 line is almost equal to that of the T line. Since the shift of the R line is expressed by a sum of positive and negative terms, the shift of the R line becomes small due to the cancellation. The shift of the S line is expected to be smaller than that of the T line, since the shift is determined by the energy denominator of the main term: 6.5 meV (the energy difference between N_1 and S) for the S line and 4.3 meV (the energy difference between N_1 and T) for the T line, respectively. The quadratic Zeeman term corresponding to the diamagnetic shift of the exciton state is considered to be very small in the present material, because of the lack of a common positive quadratic shift for the R,S, and T lines in $\mathbf{B}\parallel\mathbf{z}$ configuration. This is understandable if we consider the characteristic properties of the localized cationic exciton having a very small radius.[2]

3. *The angular dependence of the magnetic-field effect*

In the MA spectra for bulk excitons, there is no dependence on the angle θ between $\mathbf{B}$ and the crystal axis. In case of SFE's, however, the dependence on the angle θ can be clearly detected. Equation (4) describes the magnetic-field dependence and also the angular dependence of the energy shifts in a magnetic field in the $\mathbf{B}\perp\mathbf{z}$ configuration when the layer translation by the stacking fault takes place only for one direction. In the actual case, the stacking fault translational vector $\mathbf{t}$ should have the C_3 symmetry as the host crystal, so that the function $f(\theta)$ should be replaced by

$$F(\theta)=n_1 f(\theta)+n_2 f\left[\theta+\frac{2\pi}{3}\right]+n_3 f\left[\theta+\frac{4\pi}{3}\right], \tag{5}$$

where n_1,n_2, and n_3 are the number of stacking faults which occur at the three equivalent directions of $\mathbf{t}$. If the sample contained several numbers of stacking faults, the distribution of the number n_1,n_2, and n_3 may be different from sample to sample. This would give the sample-dependent shift in magnetic fields, if a certain crystalline axis is not oriented to the magnetic-field direction. When $n_1\approx n_2\approx n_3$, we can expect the most complicated structural line shape induced by this θ-dependent shift. If the distribution of the stacking fault is large for only one particular direction, a strong θ dependence for the energy shift is expected through $f(\theta)$, and a single distinct peak may be observed for each SFE line. In Fig. 4, the observed fine structures in the T, S, and N_1 lines are

attributed to this angle-dependent shift owing to the different distribution of the stacking faults. We have observed a similar sample dependence of the absorption intensities of the SFE line, correlated to the stacking fault density and the polarization at zero magnetic fields. This also confirms the above inference.

In a previous paper,[2] we presented a large angle ϕ (between **B** and **E**) dependence in both the bulk direct and indirect excitons. This dependence was understood in terms of the dipole matrix elements based on the cationic exciton model. Since the states of SFE's are composed of a linear combination of the bulk cationic states perturbed by the stacking fault effect, the angle ϕ dependence becomes more complicated than that of the bulk excitons. Overall properties of the dipole matrix elements of the SFE's have been understood by the previous measurements of the polarization dependences in the absence of magnetic field, where the direction of the transition dipole of the R exciton is normal to that of the S and T excitons: the wave function of the R exciton is x like, while that of the S and T excitons is y like.[17] Considering the distribution of stacking fault planes in the crystal, we find that the observed polarization spectra for all SFE lines comprise three superimposed components due to different dipoles with angles $\phi=0$, $2\pi/3$, and $4\pi/3$. In the presence of magnetic fields, each SFE state is mixed with other states, which leads to a more complicated ϕ-dependent spectrum. The peak positions of the split-off structures at fixed θ do not show any change when the angle ϕ is varied. However, a drastic change of the intensity is expected. This characteristic ϕ dependence is demonstrated in Fig. 5 from spectra b to e with increasing ϕ.

Starostin *et al.*[13] have also observed negative shifts in the $\mathbf{B}^2$ dependence of the T and S lines in the $\mathbf{B}\perp\mathbf{z}$ configuration. They have analyzed the results on the basis of a bielectronic diamagnetic shift, and the negative shifts in both lines have been ascribed to a negative reduced mass of $n=5$ and $n=6$ bielectron states, respectively. Recently, Röseler, Shekhmametev, and Neugebauer theoretically supported this model.[14] However, the $\mathbf{B}^2$ dependence is commonly observed not only in these lines but also in bulk excitons[2] and the other localized exciton system. Some of these states which lie at lower energies show the negative shifts with the $\mathbf{B}^2$ dependence. In SFE lines, a positive shift with $\mathbf{B}^2$ dependence is also observed for N_1, N_2, and Q lines, which has not been shown in their experimental spectra. The θ and ϕ dependences in magnetic fields cannot be explained on the basis of the bielectron model but only by the present exciton model localized at a stacking fault.

B. The magneto-absorption spectra for the *P* line

The P line shows a similar magnetic field behavior to those of the indirect excitons.[2] Thus the effect of the P state can be discussed based on the wave functions similar to the indirect state. The P lines should consist of four states as in the case of indirect excitons. We have observed P_1, P_2, and P_4 lines out of the four. Their energy positions are presented in Fig. 9 against the square of magnetic field. The unobserved line P_3 which corresponds to the ψ_3^i state of the indirect excitons can be calculated using the energy position and shift of the P_1 line with the same procedure employed in the previous paper.[2] The calculated energy of the P_3 line is plotted in Fig. 9. The four components of the P line in the $[\mathbf{B}\perp\mathbf{z}]$ configuration correspond to the four states of the cationic indirect excitons. We assigned that the P_4 is associated with ψ_4^i, P_3 with ψ_3^i, P_2 with ψ_{10}^i, and P_1 with ψ_6^i.

In the $\mathbf{B}\|\mathbf{z}$ configuration, a smaller splitting of the P line than for $\mathbf{B}\perp\mathbf{z}$ is observed. The shift is very small but has a $\mathbf{B}^2$ dependence at high magnetic field as can be seen in Fig. 9. On the basis of the cationic exciton model, the bulk exciton in the $\mathbf{B}\|\mathbf{z}$ configuration should have only diagonal Zeeman matrix elements. Thus a linear dependence on the magnetic field is expected within this model. However, as shown in the previous section, when the exciton is localized at a defect, the states may be mixed with each other by the symmetry change at the defect. As a result, nonzero off-diagonal matrix elements between the states give rise to a small $\mathbf{B}^2$ component for $\mathbf{B}\|\mathbf{z}$ in the P states as in the SFE case of the localized cationic excitons.

As mentioned before, the origin of the P line has been assigned to the exciton associated with some polytype structures contained in a very small region inside the crystal. The indirect exciton band at the zone edge folds back to the zone center by a polytype structure in the same manner as phonons. Therefore, an absorption channel of direct transition at the indirect exciton energy becomes allowed.[7] Considering the observed magnetic-field effect in conjunction with the zone folding effect, we conclude that the origin of the P line is due to the localized exciton at a defect such as 3R and 3R′ interlayer stacking disorders, which corresponds to the smallest unit of the polytype of 3R 3R′ combined structure. The localization at such a defect results in a direct type transition at an energy lower than the position of the indirect exciton. The observed energy of the P line lies roughly 0.1 meV lower than that of the indirect exciton.[8] The P line is accompanied by a no-phonon indirect exciton transition step, which starts from the indirect exciton energy E_{gx}^i with a line shape of square-root **E** dependence (in Ref. 8, Fig. 5). The absorption intensity of the no-phonon step increases with increasing number of defects. The samples with strong absorption of the P line have a tendency to show more enhanced spectra of the no-phonon step. The P line intensity is increased by applying a shear stress. This is due to the fact that the shear stress produces various defects by disturbing the layer stacking sequence in the 3R structure. This implies that the binding of the indirect exciton to the 2D defects may be very weak. A remarkable decrease of the absorption intensity with increasing temperatures is explained by the small binding energy of the P line. The linewidth of the P line is extremely narrow compared with that of the direct exciton. The width is even less than that of the SFE's. The magnetic-field effect on the P line can be interpreted by the indirect cationic exciton state weakly localized at the irregular stacking interface.

There should also exist some point defects in layered crystals. It may be expected that the point defect also

affects the exciton in layered crystals. Actually, the MA spectra for the excitons localized at the point defects have been reported.[18] The behavior in the magnetic fields was clearly different from that of the 2D defect in the present case.

IV. SUMMARY

Magneto-absorption spectra for the sharp lines observed below the indirect exciton edge in BiI_3 were measured in high magnetic fields. A remarkable anisotropy with respect to the magnetic-field configuration, a characteristic polarization dependence of the incident light, and an energy shift and growth of different split lines with $\mathbf{B}^2$ dependence were commonly observed for these lines. All these results are consistent with those of the bulk direct and indirect excitons having small radii.[2] The behavior in magnetic fields for these lines can be well explained by linear Zeeman terms in the cationic excitons perturbed by 2D defects of stacking disorders in this material.

The small radius excitons are strongly affected by the 2D defects and are easily localized around them. The degree of localization of the exciton translational motion along the direction perpendicular to the 2D plane are dependent upon the type of the stacking disorder. The degree of localization is smaller for the P line case than that for the SFE's, since the P line is observed slightly below the indirect exciton energy while SFE's are about 20 meV below it. The wave functions of the localized exciton can be well described by those of the weakly perturbed bulk cationic excitons. In a sense that the exciton localization energy is relatively small, the situation might be similar to the case of excitons bound to shallow centers in the usual semiconductors. The excitons bound to shallow donors or acceptors in semiconductors, however, usually show complicated spectra in magnetic fields due to a combined effect of the orbital component with the state of the point defect.[1] In the present case of the 2D defects, the magnetic-field effect is closely related to that of the bulk excitons. Therefore, the information on the orbital and spin states of the localized excitons, such as the g factor, may be obtained from the analysis of the bulk cationic excitons in magnetic fields, as will be discussed in a forthcoming paper.

We have also obtained detailed information on the excitons localized at the different types of the 2D defects in layered crystals in the case of the exciton having a small radius. The SFE lines arise from the exciton localized around the stacking fault produced only during the crystal growth. The stacking fault produces two kinds of deformed cell along the stacking fault plane. The cation-cation distance between the two layers becomes smaller than that of the regular arrangement of the layers. The states of the SFE's are well understood by those of the indirect excitons with a small portion of the contribution from the direct ones. As a result, alternative exciton states in the deformed cells give rise to the eight SFE states which are actually observed in the presence and absence of magnetic fields. The P line originates from the indirect exciton localized weakly at an irregular arrangement of the layer, in which the interatomic distance of the cations between two layers is not different from the regular arrangement of the layers. Only the position of the cations between the second-nearest neighbors is different from that in the regular lattice.

Systematic and precise measurements have enabled us to interpret the behavior of magneto-optical effects on these exciton lines based on a localized cationic exciton model rather than the bielectron model.

ACKNOWLEDGMENTS

The authors would like to thank Professor T. Iida for his kind discussion of this work from the theoretical point of view. Thanks are also given to Professor Y. Toyozawa and Professor T. Karasawa for their continuous encouragement of this work. This work was partially supported by a Grant-in-Aid for Scientific Research from the Ministry of Education, Science and Culture in Japan.

---

*Permanent address: Department of Physics, Faculty of Liberal Arts and Education, Yamanashi University, Takeda, Kofu 400, Japan.

[1] D. C. Reynolds and T. C. Collins, *Excitons, Their Properties and Uses* (Academic, New York, 1981), pp. 8–31.

[2] S. Takeyama, K. Watanabe, N. Miura, T. Komatsu, R. Koike, and Y. Kaifu, Phys. Rev. B **41**, 4512 (1990).

[3] Y. Kaifu, T. Komatsu, and T. Aikami, Nuovo Cimento B **38**, 449 (1977).

[4] T. Komatsu, Y. Kaifu, T. Karasawa, and T. Iida, Physica B **99**, 318 (1980).

[5] J. L. Brebner and E. Mooser, Phys. Lett. **24A**, 274 (1967); N. Kuroda and Y. Nishina, Nuovo Cimento B **32**, 109 (1976); J. J. Forney, K. Maschke, and E. Mooser, J. Phys. C **10**, 1887 (1977); X. C. Zhang, M. Gal, and A. V. Nurmikko, Phys. Rev. B **30**, 6214 (1984).

[6] Le Chi Than, C. Depeuring, F. Levy, and E. Mooser, J. Phys. Chem. Solid **36**, 699 (1975).

[7] T. Karasawa, T. Komatsu, and Y. Kaifu, Solid State Commun. **44**, 323 (1982).

[8] Y. Kaifu and T. Komatsu, J. Phys. Soc. Jpn. **40**, 1377 (1976).

[9] E. F. Gross, V. I. Perel, and R. I. Shekhmamet'ev, Pis'ma Zh. Eksp. Teor. Fiz **13**, 320 (1971) [JETP Lett. **13**, 229 (1971)].

[10] W. Czaja, G. Habeke, L. Krausbauer, E. Meier, B. J. Curtis, H. Buruner, and E. Tossati, Solid State Commun. **13**, 1445 (1973); Y. Petroff, P. U. Yu, and Y. R. Shen, Phys. Status Solidi B **6**, 419 (1974); M. P. Lisitsa, L. F. Gudymenko, F. V. Motsuyi, and D. I. Beletskan, Fiz. Tverd. Tela (Leningrad) **16**, 1965 (1974) [Sov. Phys. Solid State **16**, 1280 (1975)]; A. M. Vainrub, A. V. Iinskii, and B. V. Novikov, *ibid.* **15**, 440 (1973) [**15**, 314 (1973)].

[11] S. Tatsumi, T. Karasawa, T. Komatsu, and Y. Kaifu, Solid State Commun. **54**, 587 (1985); K. Watanabe, T. Karasawa, T. Komatsu, and Y. Kaifu, J. Phys. Soc. Jpn. **55**, 897 (1986).

[12] E. F. Gross, I. N. Uraltsev, and R. I. Shekhmamet'ev, Pis'ma Zh. Eksp. Teor. Fiz. **13**, 503 (1971) [JETP Lett. **13**, 357

(1971)].
[13]N. V. Starostin, N. I. Ulitskii, B. M. Kharlamov, and R. I. Shekhmamet'ev, Fiz. Tverd. Tela (Leningrad) **26**, 1354 (1984) [Sov. Phys. Solid State **26**, 823 (1984)].
[14]J. Röseler, R. I. Shekhmamet'ev, and J. Neugebauer, Phys. Status Solidi B **145**, 579 (1988).
[15]T. Komatsu, Y. Kaifu, S. Takeyama, and N. Miura, Phys. Rev. Lett. **58**, 2259 (1987).
[16]K. Watanabe, T. Komatsu, S. Takeyama, Y. Iwasa, N. Miura, and Y. Kaifu, J. Phys. C **20**, 6315 (1987).
[17]T. Komatsu, J. Lumin. **40&41**, 495 (1988).
[18]Y. M. Adbel Aziz and R. I. Shekhmamet'ev, Fiz. Tverd. Tela (Leningrad) **27**, 3397 (1985) [Sov. Phys. Solid State **27**, 2044 (1985)].